24 th EUROPEAN ROTORCRAFT FORUM
Marseilles, France - 15th-17th September 1998

REFERENCE: TE14

ROTOR STATE MEASUREMENTS ON THE BLACK HAWK HELICOPTER

Norman D. Ham
Massachusetts Institute of Technology
Cambridge, MA 02139

Rotor state measurements on the Black Hawk helicopter using blade-mounted accelerometers are described, beginning on the Airloads Black Hawk in 1987, then in 1994, and finally on the RASCAL - Black Hawk in 1998. The underlying theory is also presented, including a method for removing the effect of vehicle motion from the accelerometer signals.

1. INTRODUCTION

Highly agile helicopters require high-gain attitude control systems. The effect of blade dynamics must then be incorporated in the attitude control system design [1]. Therefore the measurement of blade flapping states is required. Such measurements are also required in the implementation of Individual-Blade-Control (IBC) [2].

The measurement of rotor blade flapping states on the Black Hawk helicopter using blade-mounted accelerometers was commenced in 1987 [3]. These tests demonstrated that the measurement required two accelerometers located at the blade root. This knowledge was then applied to blade flapping measurements on the Bell 412 rotor during wing tunnel tests [4] and the Airloads Black Hawk during flight tests [5].

Currently this technology is being applied to the RASCAL Black Hawk [6].

Accelerometers have also been applied to the measurement of other rotor blade states, e.g., torsion [7], lagging [8], and flatwise bending [9].

2. ACCELEROMETER KINEMATICS

From Figure 1, the blade flatwise acceleration at station due to response of the first two flatwise modes is

$$a(r) = (r\text{-}e)\,\ddot{\beta}(t) + r\Omega^2\beta(t) + \eta(r)\,\ddot{g}(t) + r\Omega^2\eta'(r)g(t)$$

Then, for accelerometers mounted at r_1, r_2, r_3, and r_4

$$\begin{bmatrix} a_1 \\ a_2 \\ a_3 \\ a_4 \end{bmatrix} = \begin{bmatrix} (r_1-e) & r_1\Omega^2 & \eta(r_1) & r_1\Omega^2\eta'(r_1) \\ (r_2-e) & r_2\Omega^2 & \eta(r_2) & r_2\Omega^2\eta'(r_2) \\ (r_3-e) & r_3\Omega^2 & \eta(r_3) & r_3\Omega^2\eta'(r_3) \\ (r_4-e) & r_4\Omega^2 & \eta(r_4) & r_4\Omega^2\eta'(r_4) \end{bmatrix} \cdot \begin{bmatrix} \ddot{\beta} \\ \beta \\ \ddot{g} \\ g \end{bmatrix}$$

In matrix notation, $A = M \cdot R$

Then the flatwise modal responses are given by

$$R = M^{-1} \cdot A$$

Note that the elements of M^{-1} are dependent only upon blade spanwise station, rotor rotation speed, and bending mode shape, i.e., they are independent of flight condition.

Since the elements of M^{-1} are independent of flight condition, the solution for a desired modal response involves only the summation of the products of spanwise accelerometer signals and their corresponding constant matrix elements by an analog or digital device, here called a solver.

Consider the block diagram shown in Figure 2. For modal acceleration $\ddot{x}$ and modal displacement x determined as above for any mode, this diagram represents the following filter equations from [10]:

$$\frac{d}{dt}\hat{\dot{x}} = \hat{\ddot{x}} + K_1(\dot{x} - \hat{\dot{x}}) \qquad (3)$$

$$\frac{d}{dt}\hat{x} = \hat{\dot{x}} + K_2(x - \hat{x}) \qquad (4)$$

where the hatted quantities are estimated values, and K_1 and K_2 are constants. Writing the estimation error as

$$e = x - \hat{x}$$

and differentiating equation (3) with respect to time, there results

$$\frac{d^2}{dt^2}\hat{x} = \frac{d}{dt}\hat{\dot{x}} + K_1\dot{e} \qquad (5)$$

Substituting equation (4) into equation (5),

$$\frac{d^2}{dt^2}\hat{x} = \ddot{x} + K_2 e + K_1\dot{e} \qquad (6)$$

Since $\frac{d^2}{dt^2}\hat{x} - \ddot{x} = -\ddot{e}$, equation (6) becomes

$$\ddot{e} + K_1\dot{e} + K_2 e = 0 \qquad (7)$$

This expression represents the dynamics of the estimation error. The corresponding characteristic equation is

$$s^2 + K_1 s + K_2 = 0$$

The bandwidth and damping of the estimation process are determined by the choice of the constants K_1 and K_2.

Since the elements of the filter shown in Figure 2 are independent of flight condition, the estimation of modal rate response involves only the integration of the products of constants and the measured modal responses by an analog or digital device, here called a McKillip filter. Note that an improved estimate of the modal displacement x is also obtained due to the double integration of modal acceleration $\ddot{x}$ embodied in the filter. Also, note that no knowledge of the rotor or its flight condition is required in designing the filter.

3. REMOVING THE EFFECTS OF VEHICLE MOTION

Flight tests have shown that a considerable portion of blade-mounted accelerometer signals is due to vehicle motion during maneuvering flight.

The purpose of this investigation is to identify the signal components due to vehicle motion, and determine a means of eliminating them from the accelerometer signals.

Consider the inertial axis system shown in Figures 3 and 4. Blade flapping with respect to the X-Y (inertial) plane is

$$\beta_{IP} = \beta_0 + (\beta_{1_c} - \theta)\cos\psi + (\beta_{1_s} - \varphi)\sin\psi \qquad (1)$$

where θ and φ are fuselage Euler angles, ψ is blade azimuth Ωt, and β_0, β_{1_c} and β_{1_s} are components of flapping with respect to the hub plane, i.e.,

$$\beta_{HP} = \beta_0 + \beta_{1_c}\cos\psi + \beta_{1_s}\sin\psi \qquad (2)$$

Differentiating equation (1) with respect to time,

$$\dot{\beta}_{IP} = \dot{\beta}_0 + (\dot{\beta}_{1_c} - \dot{\theta})\cos\psi - (\beta_{1_c} - \theta)\,\Omega\sin\psi + (\dot{\beta}_{1_s} - \dot{\varphi})\sin\varphi + (\beta_{1_s} - \varphi)\,\Omega\cos\psi \qquad (3)$$

Blade inertial flapping β_{IP} and flapping velocity $\dot{\beta}_{IP}$ can be obtained using the methods of Section 2. The quantities β_0, $(\beta_{1_c} - \theta)$, and $(\beta_{1_s} - \varphi)$ can be transferred to the fixed system using the coordinate transformation described in Ref. 4 and shown in Figure 5. The quantities $\dot{\beta}_0$, $(\dot{\beta}_{1_c} - \dot{\theta})$, and $(\dot{\beta}_{1_s} - \dot{\varphi})$ can be transferred to the fixed system as shown in Ref. 4, and in Figure 6.

Then the desired quantities β_{1_c}, β_{1_s}, $\dot{\beta}_{1_c}$ and $\dot{\beta}_{1_s}$ can be obtained using the measured fuselage quantities θ, $\dot{\theta}$, φ and $\dot{\varphi}$.

4. AIRLOADS BLACK HAWK FLIGHT TESTS IN 1987 [3] AND 1994 [5]

The objective of the flight measurements was to compare flapping estimated using the root and tip acceleration measurements with that predicted by a simple rigid-blade model, and with that measured by a root-mounted flapping transducer.

Time histories and frequency spectra of the two accelerometers for an 80 kt. level flight trim condition of the UH-60A helicopter, Figure 7, are shown in Figures 8 and 9. Multiple harmonics of rotor speed (4.3 Hz) are evident in the record, with 1P and 3P contributions being particularly strong. In order to estimate flapping for purposes of controlling flight dynamics, only the lower frequency responses at 0-1P are of interest. The analysis of [3] indicated significant 1P tip accelerometer response due to bending contributions to the local values of blade slope and blade acceleration, which together determine the tip accelerometer response. This was not the case for the root accelerometer.

The results suggested that blade 0-1P flapping estimation can be accomplished by using two inboard accelerometers to minimize the blade bending contribution to the accelerometer signals. Alternatively, the blade flapping and bending response can be determined by using four spanwise accelerometers and the methodology of Section 2 to solve for flapping and/or bending response.

The knowledge obtained from this test led to the use of two blade-root-mounted accelerometers in the wind tunnel and flight tests described in [4] and [5].

Typical Black Hawk flight test results are shown in Fig. 10.

5. RASCAL BLACK HAWK

A general description of the RASCAL helicopter is given in [6]. A *similar helicopter is shown in Fig. 7.*

The complete rotor state measurement and estimation system installed on the RASCAL is shown in Figure 11. The hub mounted LASER sensors and blade mounted accelerometers provide redundant and complementary flap and lead-lag information for the estimation algorithms. A LASER sensor is also used to measure blade pitch angle. Main rotor RPM is sensed in the fixed frame and used in the modal transformations of the accelerometer signals to produce blade angle estimates. Main rotor azimuth is also *measured in the fixed frame* for use in the multiblade coordinate transformation of the rotating system data into the non-rotating frame.

LASER distance sensors are used to estimate the flap, lead-lag, and pitch angular displacements of each main rotor blade. These sensors calculate distance from beam reflection, are highly accurate, and have a very high bandwidth. The sensors are mounted on the hub and measure displacements of the attachment spindle and pitch link which are functions of the desired angles. Since the blade is rigidly attached to the spindle, blade root angles can be inferred from these motion data. A detailed description of the LASER system is given in [11].

Two pairs of linear accelerometers are mounted on *the surface of each* blade at the locations shown in Figure 12 for the estimation of blade root flap and lead-lag angles. One pair are located with the sensitive axis perpendicular to *the plane formed by the* blade chord and span to sense blade flapping and one pair are oriented with the sensitive axis along the blade chord to sense lead-lag. The inboard member of each pair is located 27 inches from the center of the main rotor shaft. The outboard member of each pair is located 42 inches from the center of the main rotor shaft. The flapwise accelerometers are located on the upper surface of the blade at the quarter chord. The lagwise accelerometers are located on the trailing edge cutout surface.

Typical flight test data are as shown in Figure 10.

6. CONCLUDING REMARKS

The unique characteristics of blade-mounted accelerometers are as follows:

1. Their functional relationship with blade accelerations and displacements is independent of flight condition.
2. They permit an inner feedback control loop around each blade in the rotating system. Complete vehicle functions can be achieved by outer loops, which can operate at high gain, since blade stability is ensured by the inner loop.
3. They offer advantages over other sensors: the accelerometer signal can be integrated once and twice to obtain high-fidelity rate and displacement estimates.
4. *They permit control in the time-domain: this eliminates* the need for harmonic analysis found in HHC systems, with corresponding lags, and inability to follow the rapid transients found in helicopter maneuvering flight. Also, the stabilization of various blade modes becomes possible.

These unique characteristics of accelerometers make them superior blade-mounted sensor candidates for the upcoming IBC Black Hawk described in [12].

ACKNOWLEDGMENTS

The author wishes to acknowledge Ames Research Center, NASA, for financial support.

The author is grateful to Carolyn Fialkowski for her expert and patient typing of the paper.

REFERENCES

1. Ellis, C.W., "Effect of Articulated Rotor Dynamics on Helicopter Automatic Control System Requirements," Aeronautical Engineering Review, 12, 7, July 1953.

2. Ham, N.D., "Helicopter Individual-Blade-Control: Promising Technology for the Future Helicopter," Proc. AHS Aeromechanics Specialists Meeting, Bridgeport, CT, October 1995. Also 21st European Rotorcraft Forum, St. Petersburg, Russia, Aug. 30 - Sept. 1, 1995.

3. Ham, N. D.; Balough, D.L.; and Talbot, P.D., "The Measurement and Control of Helicopter Blade Modal Response Using Blade-Mounted Accelerometers," Proc. Thirteenth European Rotorcraft Forum. September, 1987.

4. Ham, N.D., and McKillip, R.M. Jr., "Research on Measurement and Control of Helicopter Rotor Response Using Blade-Mounted Accelerometers 1990-91," Proc. 17th European Rotorcraft Forum, Berlin, Germany, September 1991.

5. Balough, D.L., "Estimation of Rotor Flapping Response Using Blade-Mounted Accelerometers," Proc. AHS Aeromechanics Specialists Conference, San Francisco, California, January 1994.

6. Jacobsen, R.A., Rediess, N.A., Hindson, W.S., Aiken, E.W., and Bivens, C.C., "Current and Planned Capabilities of the NASA/Army Rotorcraft Aircrew Systems Concepts Airborne Laboratory (RASCAL)," Proc. of the 51st Annual Forum of the AHS, Fort Worth, TX, May 1995.

7. Ham, N.D. and Quackenbush, T.R., "A Simple System for Helicopter Individual-Blade-Control and Its Application to Stall-Induced Vibration Alleviation," Proc. AHS National Specialists' Meeting on Helicopter Vibration, Hartford, CT, November 1981. Also, Proc. of the Seventh European Rotorcraft Forum, Garmisch-Partenkinchen, Germany, September 1981.

8. Ham, N.D., and McKillip, R.M. Jr., "Research on Measurement and Control of Helicopter Rotor Response Using Blade-Mounted Accelerometers 1991-92," Proc. 18th European Rotorcraft Forum, Avignon, France, September 1992.

9. Ham, N.D., and McKillip, R.M., Jr., and Balough, D.L., "Research on Measurement and Control of Helicopter Rotor Response Using Blade-Mounted Accelerometers 1992-93," Proc. Nineteenth European Rotorcraft Forum, Como, Italy, September 1993.

10. McKillip, R.M., Jr., "Periodic Control of the Individual-Blade-Control Helicopter Rotor," Vertica, 9, 199-224, 1985.

11. Fletcher, J.W., and Tischler, M.B., "Improving Helicopter Flight Mechanics Models Using LASER Measurements of Blade Flapping," Proc. 53rd Annual National Forum of the American Helicopter Society, Virginia Beach, VA, April 1997.

12. Jacklin, S., "RADICL Program Review," unpublished communication, February, 1998.

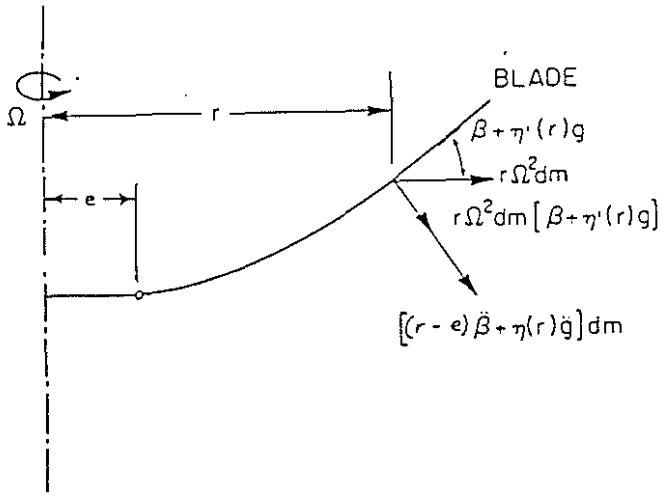

Figure 1. Blade Flatwise Inertia Forces

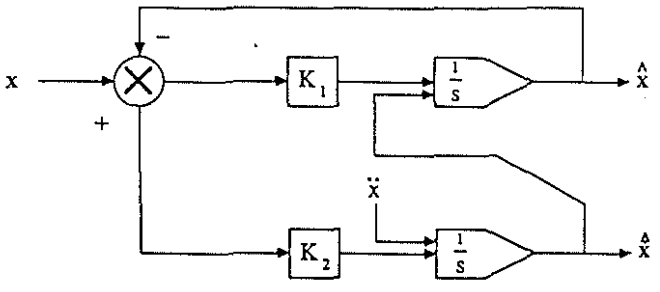

Figure 2. Block Diagram of McKillip Filter

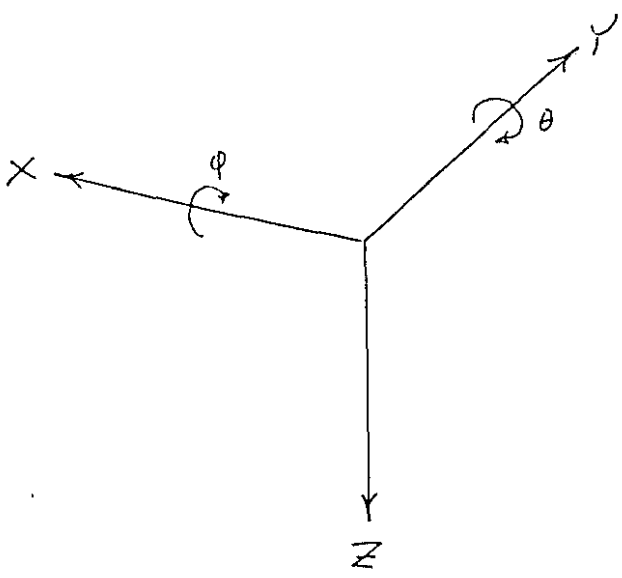

Figure 3. Helicopter Inertial Axes

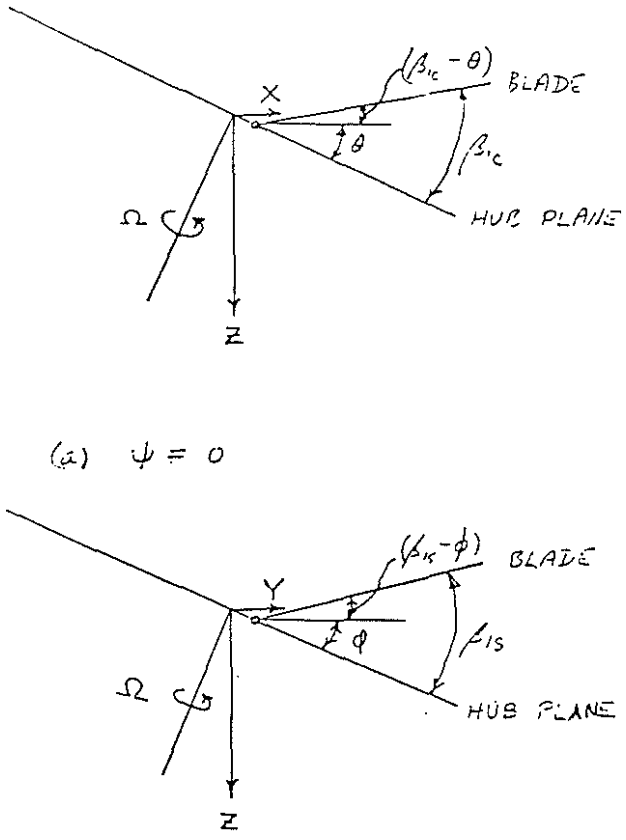

Figure 4. Blade Flapping Geometry

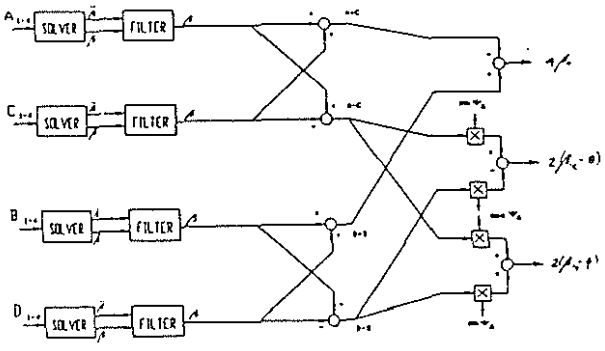

Figure 5. Schematic of Flapping Displacement Measurement System ($\beta \triangleq \beta_{1P}$)

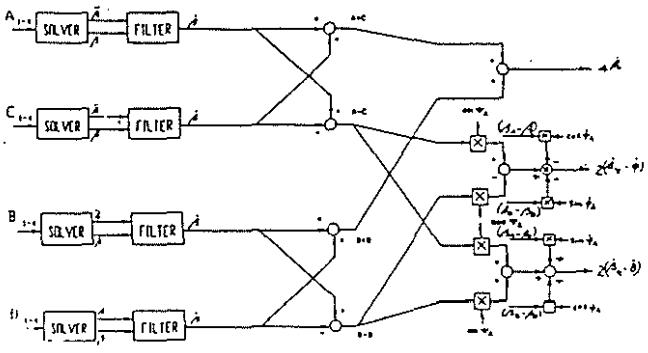

Figure 6. Schematic of Flapping Rate Measurement System ($\beta \triangleq \beta_{1P}$)

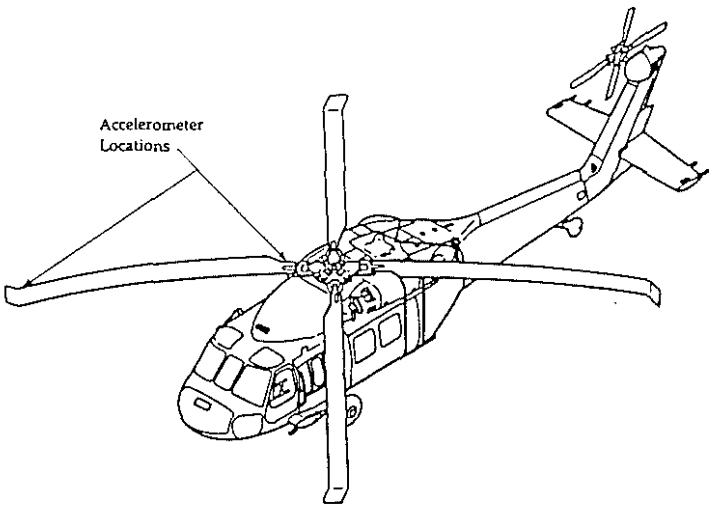

Figure 7. The Sikorsky Black Hawk Helicopter

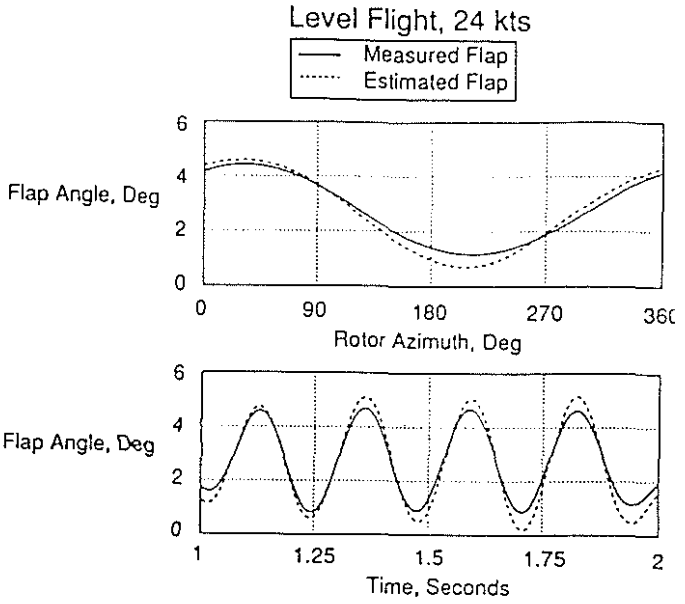

Figure 10. Blade Flapping in Forward Flight

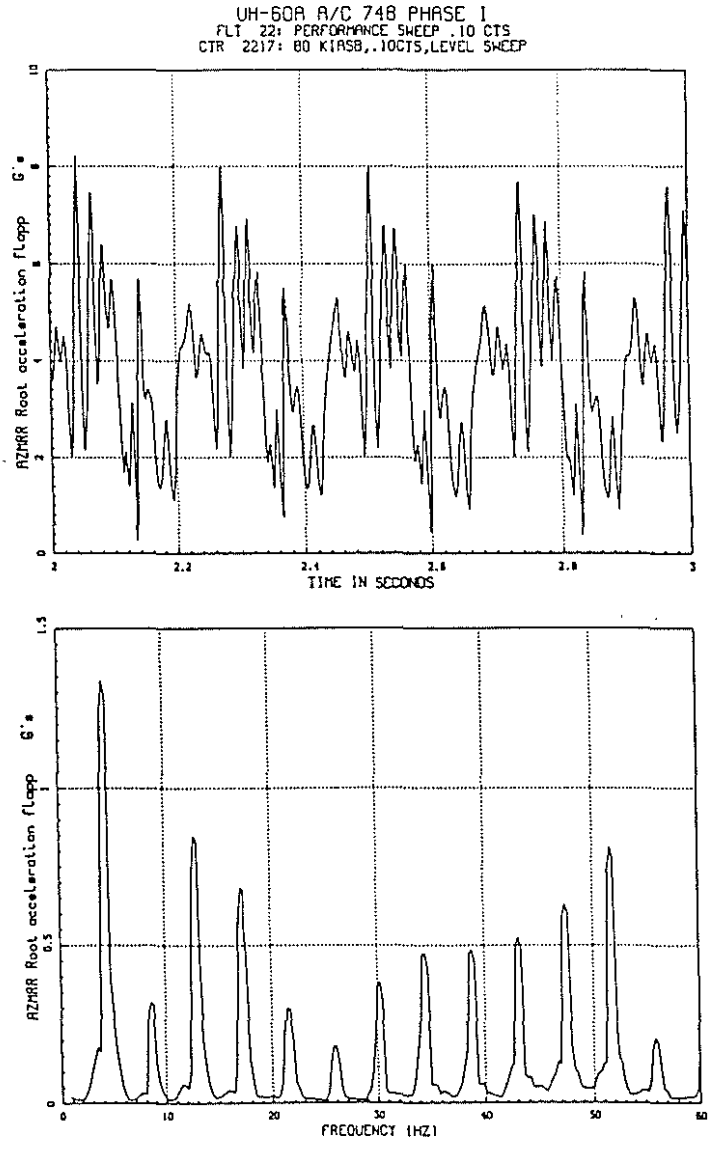

Figure 8. Root Accelerometer Time History and Frequency Spectrum

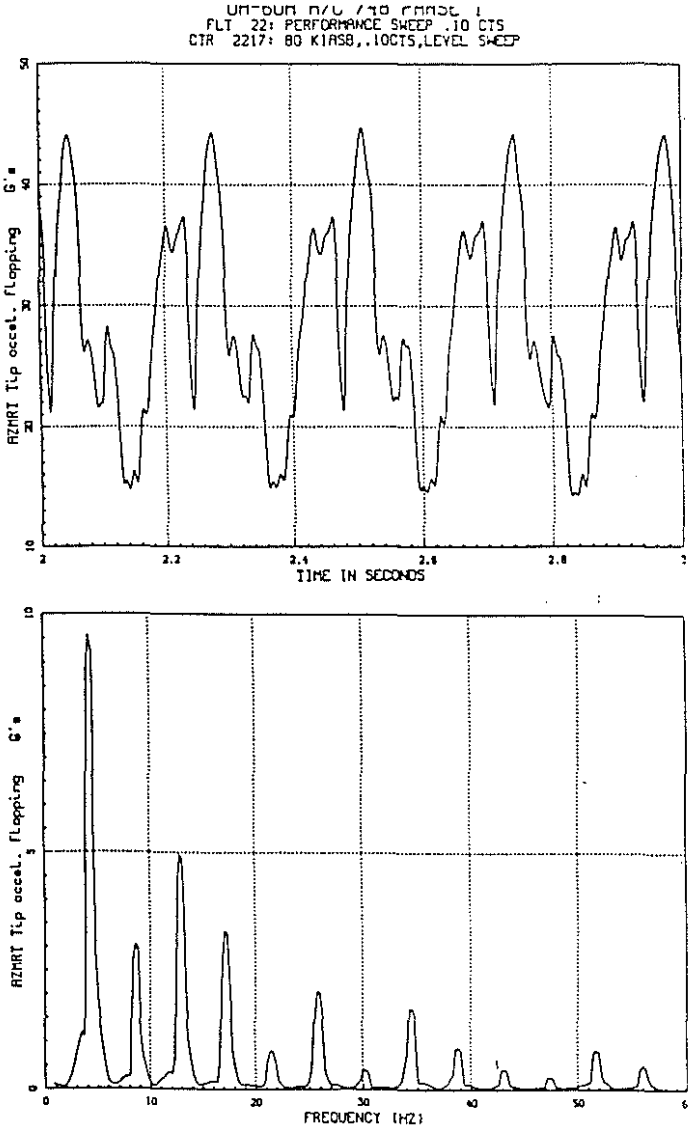

Figure 9. Tip Accelerometer Time History and Frequency Spectrum

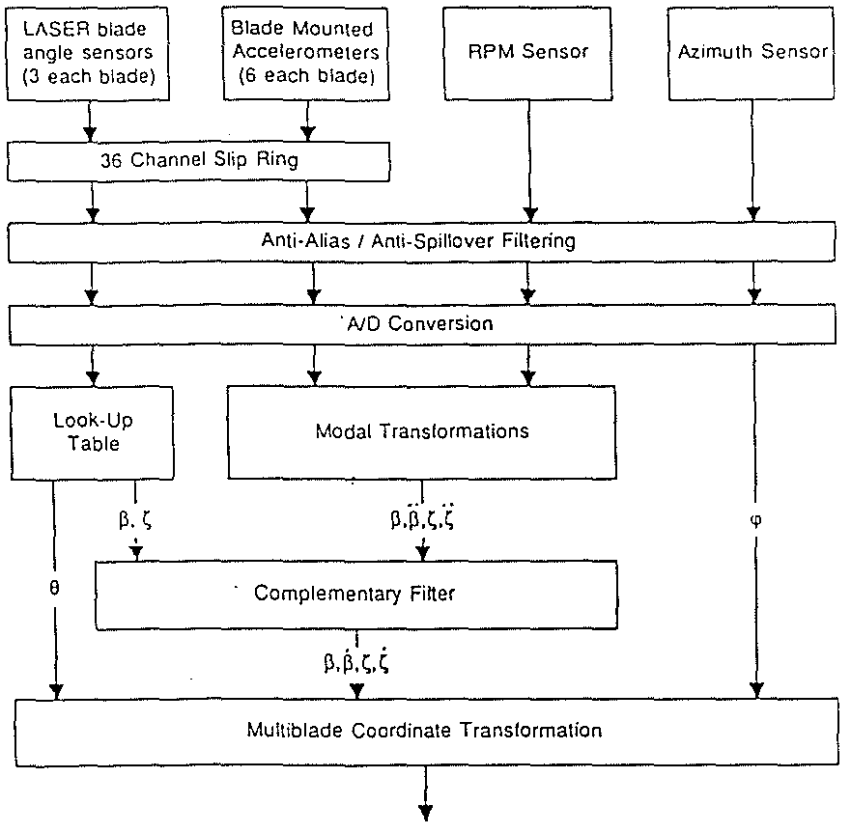

Figure 11. Schematic of RASCAL Blade Instrumentation

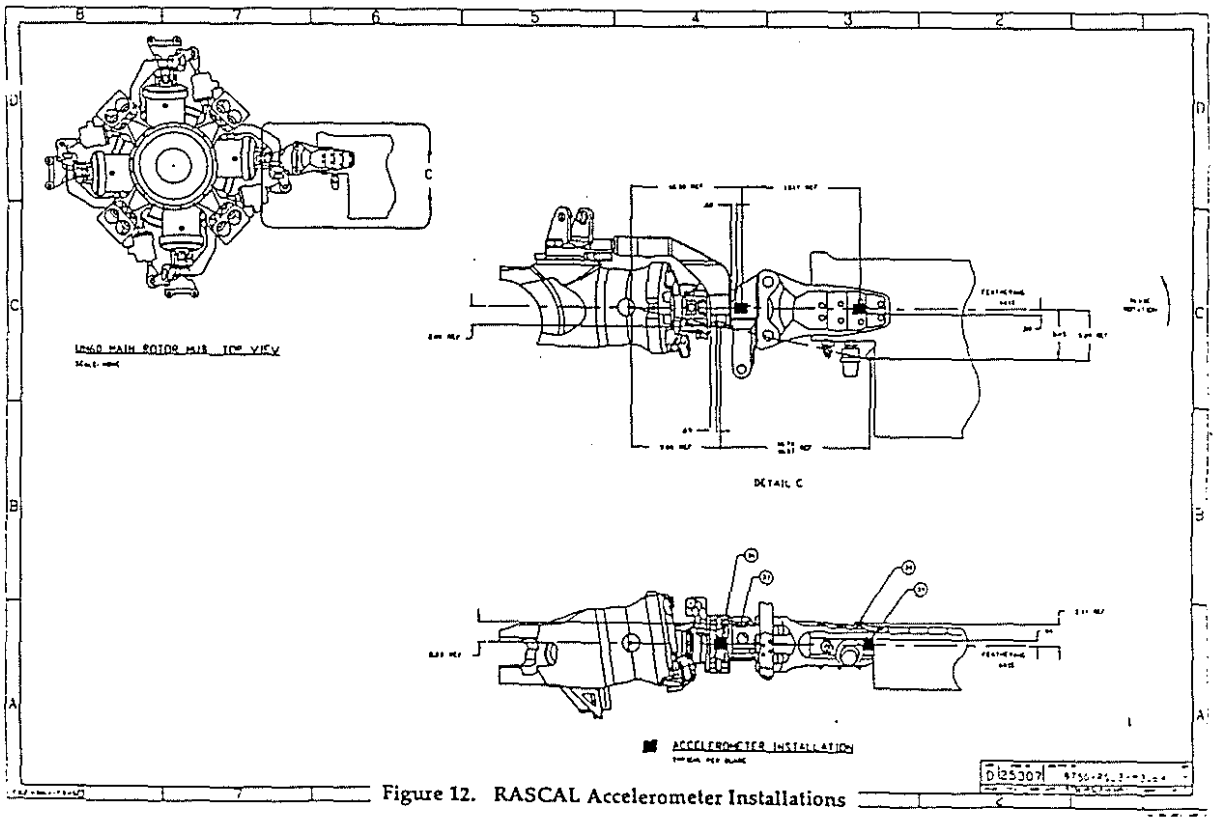

Figure 12. RASCAL Accelerometer Installations